Identification of Novel Peptide Binding Proteins in the Endoplasmic Reticulum: ERp72, Calnexin, and grp170[†]

Pieter Spee,[‡] John Subjeck,[§] and Jacques Neefjes*,[‡]

Division of Tumor Biology, Netherlands Cancer Institute, Amsterdam, The Netherlands, and Department of Molecular and Cellular Biology, Roswell Park Cancer Institute, Buffalo, New York 14263

Received February 9, 1999; Revised Manuscript Received May 10, 1999

ABSTRACT: Transient interactions between molecular chaperones and nascent polypeptide chains assist protein folding in the endoplasmic reticulum. In an experimental setting that resembles the ER, we have used peptides as model substrates to identify and compare substrate specificities of ER-resident chaperones. The ER-located peptide transporter TAP was used to introduce peptides into the lumen of microsomes. In addition to PDI and gp96, previously identified as peptide-binding chaperones in the ER, we show that ERp72, calnexin, and grp170 interact with TAP-translocated peptides. The chaperones that have been identified can all bind peptide substrates that range from 8 to 40 amino acids in a manner independent of ATP. In addition, these chaperones exhibit broad and largely overlapping, however not identical, substrate selectivities. Our data indicate that peptide translocation into microsomes via TAP can be used as a method to monitor substrate selectivities of ER-resident chaperones. The implications of the observed preferences for chaperone−substrate interactions and for chaperones applied as vehicles in peptide-based vaccination strategies will be discussed.

The endoplasmic reticulum (ER)[1] is a site of constant import and export of (poly)peptides. A continuous flow of nascent proteins enters the ER lumen cotranslationally via the sec61p complex (*1*). Here, the redox potential of the ER environment and transient interactions with multiple chaperones ensure that proteins fold correctly. Smaller peptides [8−40 amino acids (*2*−*5*)], predominantly the products of protein turnover by the 26S proteasome (*6*), are introduced into the ER lumen via the transporter associated with antigen processing (TAP) (*7*−*9*). Here, a subset of the TAP-translocated peptides can bind MHC class I molecules. In addition, a fraction of TAP-translocated peptides has been found in association with ER-resident chaperones, both in vivo (*10*) and in vitro (*11*−*14*). These include gp96, protein disulfide isomerase (PDI), calreticulin, and two as yet unidentified proteins of 120 and 170 kDa.

Molecular chaperones, which include many heat-shock or stress proteins, are a group of functionally related proteins that are found in various organelles throughout the cell. They assist protein folding, but stabilize mature proteins as well. Despite the physical interaction with their substrates, presumably to prevent nonspecific aggregation of (partially) unfolded polypeptides, chaperones do not form a functional part of the final protein. In the ER, a cellular compartment specialized in the production and secretion of proteins, the different chaperones form a major constituent. Their assistance in ER protein folding has been studied extensively, both in vitro and in vivo. For example, well established is the role of chaperones in the formation of heterotrimeric MHC class I molecules, from a heavy chain (H-chain), β2-microglobulin (β2m), and a peptide of around 9 amino acids (*15*, *16*). The initial folding of the intermediate H-chain−β2m heterodimer is promoted by the membrane-bound chaperone calnexin (*17*), followed by its soluble homologue calreticulin, thioredoxin-like ERp57 (*18*−*20*), and the MHC class I specialized chaperone tapasin (*21*, *22*). After antigenic peptides bind, these chaperones are released and the functional class I heterotrimer is transported to the cell surface (*23*).

The relatively oxidizing environment of the ER lumen and its N-glycosylation machinery directly affect protein folding, i.e., as reflected in the formation of disulfide bridges. In addition, it may influence the interaction between chaperones and their substrates, which is essential for chaperones to support protein folding. Two major classes of ER-resident chaperones have been defined: lectin-like chaperones, recognizing monoglucosylated N-linked glycans [i.e., calnexin and calreticulin (*24*−*26*), reviewed in ref *27*], and chaperones recognizing unfolded protein stretches [e.g., BiP, which recognizes alternating hydrophobic X sequences (*28*, *29*), and PDI (*30*, *31*)]. However, the substrate binding specificities of most ER-resident chaperones, like gp96, have been poorly characterized as yet. In addition, little is known about the relative capacities of chaperones to bind peptides

[†] This research is supported by Netherlands Organization for Scientific Research (NWO) Grant 901-09-228 and Dutch Cancer Society (NKB) Grant 95-982.

* To whom correspondence should be addressed: The Netherlands Cancer Institute, Plesmanlaan 121, 1066CX Amsterdam, The Netherlands. Telephone: +31-20-5121977. Fax: +31-20-5122029. E-mail: jneefjes@nki.nl.

[‡] Netherlands Cancer Institute.

[§] Roswell Park Cancer Institute.

[1] Abbreviations: BiP, immunoglobulin heavy chain binding protein; Bpa, *p*-benzoylphenylalanine; ER, endoplasmic reticulum; gp, glycoprotein; grp, glucose-regulated protein; hsp, heat shock protein; MHC, major histocompatibility complex; PDI, protein disulfide isomerase; TAP, transporter associated with antigen processing.

10.1021/bi990321r CCC: $18.00
Published on Web 07/21/1999

within the environment of the ER. Yet such interactions are currently applied in peptide-based vaccination strategies, since not only peptide-associated gp96, but also cytosolic chaperones, were shown to protect mice against the same tumor from which it was derived (*32*−*35*).

Here, we have used the largely nonselective substrate activity of rat TAP1/2[a] (*36*, *37*), to introduce different sets of 8−40mer peptides as substrates for ER-resident chaperones, (1) to identify the as yet unidentified peptide-binding proteins of 120 and 170 kDa and (2) and to study substrate-specific interactions of these ER-resident chaperones. Peptide translocation via TAP is ER-restricted and therefore allows the study of peptide−chaperone interactions in crude microsomes, which in vitro form a proper environment for ER protein folding. To visualize peptide−protein interactions, we have used radioiodinated peptides that contain the photoreactive group *p*-benzoylphenylalanine (Bpa), which converts into a covalent linker upon UV irradiation (*38*). These peptides allow the analysis and identification of peptide−protein interactions by two-dimensional IEF/SDS−PAGE followed by Western blotting, and enable a direct comparison of (poly)peptide-binding capacities in the ER. Besides PDI and gp96, the peptide-binding proteins of 120 and 170 kDa were identified as the ER-resident chaperones calnexin and grp170, respectively. In addition, we show that the PDI-related protein ERp72 is an acceptor of TAP-translocated peptides in the ER, albeit with binding characteristics different from those of PDI. Notably, grp170 appears to bind peptides very efficiently. As may be expected for chaperones, the length of the peptide substrate (8−40 amino acids) does not restrict binding to the peptide-binding proteins that were studied. However, the various chaperones differ in their relative extent of binding of different peptide substrates. The off-rate of peptides appears to be ATP-independent for all the chaperones that were studied and is relatively slow for PDI which may explain why this chaperone is the most dominant peptide acceptor in the ER. We here describe an experimental model for analysis of (peptide) substrate specificities of ER chaperones, which may have important implications for both protein folding and the development of peptide chaperone-based vaccines.

MATERIALS AND METHODS

Antibodies. Rabbit polyclonal antiserum against grp170 was generated against purified Chinese hamster grp170 (*39*). The rat monoclonal antibody SPA850, directed against human gp96, was purchased from StressGen (Victoria, BC). The monoclonal antibody AF8, directed against calnexin (*40*), was a kind gift of J. Borst (NKI, Amsterdam, The Netherlands). The polyclonal antibody against the C-terminus of murine ERp72 was a kind gift of M. Green (St. Louis University, St. Louis, MO). Murine monoclonal antibodies against human PDI were obtained from ABR (Golden, CO).

Cell Lines. Cell line T2 is a human TAP-deficient TxB hybrid (*41*). T3 is a T2-derived cell line stably transfected with rat TAP1 and TAP2[a] (*42*). Both cell lines were cultured in Hepes-buffered RPMI 1640 medium supplemented with 8% FCS.

Peptides. All photoreactive peptides were synthesized by f-moc chemistry using a Millipore 9050 Plus PepSynthesizer and include a tyrosine (Y) for iodination and the photoreactive amino acid analogue BPA (Bachem AG, Bubendorf, Switzerland). All peptides have a free carboxy terminus and were more than 90% pure as determined by HPLC analysis. The peptides that were used are listed in Table 1.

Table 1: List of Peptides

	code	sequence		code	sequence
1	5PS1	ERYNKSE-[BPA]-L	7	6PS2H	Y-[X]37-[BPA]-K[a]
2	5PS2	ERYDKSE-[BPA]-L	8	6PS3	YF-[X]4-[BPA]-XF[b]
3	6PS2A	Y-[X]5-[BPA]-K[a]	9	6PS4	YL-[X]4-[BPA]-XL[b]
4	6PS2C	Y-[X]7-[BPA]-K[a]	10	6PS5	YK-[X]4-[BPA]-XK[b]
5	6PS2E	Y-[X]11-[BPA]-K[a]	11	6PS6	YD-[X]4-[BPA]-XD[b]
6	6PS2F	Y-[X]17-[BPA]-K[a]	12	6PS7	YT-[X]4-[BPA]-XT[b]

[a] X is a degenerated mixture of K, D, T, A, and F. [b] X is a degenerated mixture of K, D, T, L, and F.

Peptides were ^{125}I-labeled by iodogen (Pierce)-catalyzed iodination, and free iodine was removed using either Sephadex G10 or Sepak columns (specific activity of 20−50 mCi/mg of peptide). During synthesis and iodination, the peptides were protected from light exposure. Peptides were stored in PBS at −20 °C in the dark.

Preparation of Microsomes. Microsomes were prepared as described previously (*43*). Briefly, 2.5×10^9 cells were washed in STKMM buffer [250 mM sucrose, 50 mM TEA-HCl (pH 7.5), 50 mM KAc, 5 mM $MgAc_2$, 0.1% β-mercaptoethanol, and 10 mg/mL PMSF]. The cell pellet was resuspended in H_2O and homogenized with a tight fitting douncer. After centrifugation of the homogenate for 10 min at 7500 rpm (Beckman SS34 rotor, 4 °C) to remove cellular debris, the supernatant was spun at 18 000 rpm for 40 min. The microsomal pellet was washed once with STKMM buffer by resuspending the pellet with a douncer, and subsequent centrifugation (18 000 rpm for 40 min at 4 °C). Finally, the microsomes were taken up in PBS, snap-frozen (corresponding to microsomes of 1.5×10^6 cells/mL), and stored at −80 °C. The integrity of the microsomes was tested as described previously (*14*).

Peptide Translocation and Photoaffinity Labeling. Microsomes generated from 5×10^7 cells were incubated in incubation buffer [130 mM KCl, 10 mM NaCl, 1 mM $CaCl_2$, 2 mM EGTA, 2 mM $MgCl_2$, and 5 mM Hepes (pH 7.3)] with 2 mg of radioiodinated peptides in the presence of 10 mM Tris-buffered ATP (pH 7.0) in a final volume of 1 mL (15 min at 37 °C). To prevent further translocation and release of peptides from the ER, reaction mixtures were transferred to ice before free untranslocated peptides were removed by pelleting (14 000 rpm for 5 min at 4 °C) and subsequent washing with ice-cold incubation buffer. All reactions were performed in the dark. Photoaffinity labeling was initiated by exposing the samples to UV light (UVP Blak-Ray B100A with Sylvania Par 38 mercury lamp) at a distance of 2 cm for 5 min on ice.

In peptide off-rate experiments, microsomes were washed after import of peptide 5PS2 and chased for various periods of time at 37 °C, either in the absence or in the presence of 10 mM ATP. After removal of released substrates, samples were photoaffinity labeled as described above and proteins separated by SDS−PAGE.

For separation of proteins by two-dimensional (2D) IEF/SDS−PAGE, microsomes were dissolved in IEF sample buffer [9.5 M urea, 2% (v/v) NP-40, 2% (v/v) ampholyte (pH 3.5−10) (Pharmacia, Uppsala, Sweden), and 5% (v/v) β-mercaptoethanol] and the proteins separated by 2D-IEF/

SDS−PAGE. Microsomal proteins were either silver-stained (Bio-Rad, Hercules, CA), Coomassie-stained, or Western-blotted, prior to visualization of the peptide-bound proteins with a Fujix BAS 2000 phosphoimager. Quantifications of peptide binding were performed using TINA 2.09 software (Raytest), and corrected for background staining by subtracting the signal of a similar area without radioactive spots in the close proximity of the quantitated signal.

For the relative expression patterns of T3 proteins, a Coomassie-stained 2D-IEF/SDS−PAGE gel was scanned and quantified using TINA 2.09 software (Raytest) in a manner similar to that described above. Indicated expression levels, which have been corrected for molecular weights, are the average of two independent analyses.

To inhibit peptide binding to PDI, T3 microsomes were preincubated at room temperature for 10 min with DMSO-dissolved β-estradiol at a final concentration of 10 mM (1 mM stock), prior to peptide translocation and photoaffinity labeling. The presence of β-estradiol was maintained throughout the different steps of the reaction. As a control, experiments were performed in the presence of an equal volume of DMSO.

Western Blotting. Proteins were transferred from polyacrylamide gels to nitrocellulose filters (Schleicher & Schuell, Dassel, FRG) and, after blocking with 0.5% (w/v) skimmed milk powder, probed with various antibodies in the presence of 1% (w/v) milk powder. Probed proteins were visualized by incubation with peroxidase-coupled second antibodies (DAKO, DK), followed by ECL chemiluminescence (Amersham) and autoradiography.

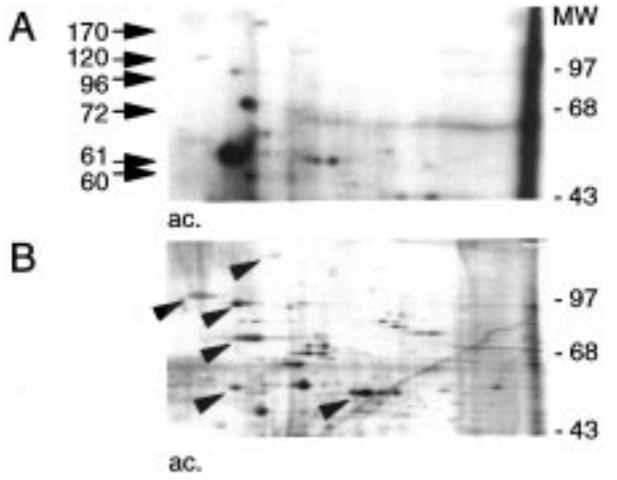

FIGURE 1: Visualization of ER-resident peptide-binding proteins after peptide translocation via TAP. (A) T3 microsomes were incubated with photoaffinity-labeled radioiodinated peptides (5PS1 being ERYNKSE-Bpa-L) in the presence of ATP for 15 min at 37 °C. Untranslocated peptides were removed and the microsomes UV-exposed to covalently link peptides with associated proteins. Following lysis, the microsomal proteins were separated by 2D-IEF/SDS−PAGE and subsequently transferred to nitrocellulose. The photoaffinity-labeled proteins were visualized by phosphoimaging. Various peptide-binding proteins were observed in microsomes with approximate molecular masses of 60, 61, 72, 96, 120, and 170 kDa, as indicated. The position of the molecular mass marker is indicated on the right (MW in kilodaltons). The acidic site of the gel is denoted ac. (B) Separation of T3 microsomal proteins by 2D-IEF/SDS−PAGE followed by silver staining. Various spots that correspond to the photoaffinity-labeled proteins shown in figure A are denoted with arrowheads.

RESULTS

TAP-Dependent Photoaffinity Labeling of ER-Resident Proteins. The peptide transporter TAP translocates peptides from the cytosol into the ER lumen in an ATP-dependent fashion (*7*, *8*, *44*). In addition to MHC class I molecules, TAP-translocated peptides, which may be considered small stretches of unfolded proteins, can associate with various ER chaperones (*12*−*14*). We have used the activity of TAP to introduce peptides into the ER lumen, as substrates to identify and compare substrate-specific interactions of ER-resident chaperones.

Calreticulin, which specifically binds glycosylated peptides, PDI, gp96, and at least two unidentified proteins with apparent molecular masses of 120 and 170 kDa were previously been found to interact with peptides in the ER (*12*−*14*, *45*). To identify the 120 and 170 kDa proteins, microsomes derived from T3 cells were incubated with radioiodinated peptide 5PS1 in the presence of ATP. This 9mer peptide has incorporated the photoreactive amino acid analogue *p*-benzoylphenylalanine (Bpa) that allows covalent photoaffinity labeling upon UV exposure. After incubation, free peptides were removed and the microsomes exposed to UV light to induce a covalent interaction between TAP-translocated peptides and associated proteins. The microsomal proteins were then separated by 2D-IEF/SDS−PAGE, followed by a transfer to nitrocellulose for immunodetection.

A set of photoaffinity-labeled proteins was detected by autoradiography, with approximate molecular masses of 60, 72, 96, 120, and 170 kDa (Figure 1A). Similar reactions with microsomes derived from TAP-deficient T2 cells revealed that peptide binding to these proteins depends on the presence of TAP (data not shown and refs *12*−*14*). This indicates that the observed peptide−protein interactions take place in the lumen of the ER and excludes the possibility that peptide binding occurs nonspecifically postlysis. Analysis of T3 microsomal proteins by 2D-IEF/SDS−PAGE, followed by silver staining, showed a large set of well-separated proteins. Only a few of these proteins were photoaffinity labeled (compare panels A and B of Figure 1; arrows in panel B denote the corresponding photoaffinity-labeled proteins of panel A), which implies that the observed interactions between peptides and microsomal proteins are selective.

Identification of the 120 and 170 kDa Peptide-Binding Proteins as Calnexin and grp170. Analyses of the peptide-binding proteins in a similar photoaffinity labeling experiment revealed that the 96, 120, and 170 kDa peptide-binding proteins correlate with relative abundantly expressed proteins, as shown by a silver-stained 2D-IEF/SDS−PAGE gel of T3 microsomal proteins (Figures 1B and 2A). To determine the identity of these proteins, a part of the Western blot, as shown in Figure 1, containing the 96, 120, and 170 kDa photoaffinity-labeled proteins was probed with antibodies against candidate proteins (Figure 2B,C).

Probing the filter with specific monoclonal antibodies confirmed the identity of the 96 kDa photoaffinity-labeled protein, as the previously identified peptide-binding protein gp96 (*11*, *12*, *14*). The 170 kDa protein was found to comigrate exactly with the ER-luminal glycoprotein grp170 (*39*). grp170 is a member of the stress-inducible HSP70 family (*46*, *47*), and was recently shown to play a role in sec61p-mediated import of nascent proteins (*48*).

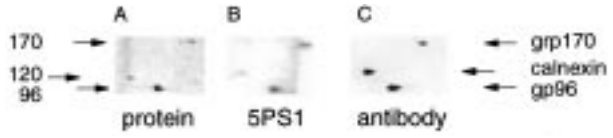

FIGURE 2: Identification of calnexin and grp170 as ER-resident peptide-binding proteins. As denoted with arrows, T3 cells ubiquitously express the 96, 120, and 170 kDa peptide-binding proteins, as visualized by silver staining (panel A, protein). The part of the Western blot shown in Figure 1A, containing the 96, 120, and 170 kDa photoaffinity-labeled proteins (panel B, 5PS1), was excised and probed with antibodies against candidate proteins. The 96 kDa protein was identified as gp96. The 120 and 170 kDa peptide-binding proteins were identified as calnexin and grp170, respectively (panel C, compilation of the three antibody signals). The identities of the different proteins are listed on the right.

The 120 kDa protein exactly comigrated with the single spot of the lectin-like chaperone calnexin. Surprisingly, calnexin, which has an estimated molecular mass of 64 kDa, migrates at a position with a higher molecular mass than gp96. This may be due to its high content of positively charged amino acids and consequently decreased level of SDS binding which retards its migration by SDS−PAGE. Calnexin is believed to be directly involved in protein folding (*49*). Like gp96 and grp170 (*50*), calnexin is found in chaperone networks that may play a role in the "quality-control" apparatus by retaining incorrectly folded proteins in the ER (*51*, *52*).

ERp72 Is an Acceptor for TAP-Translocated Peptides. In Figure 1, a dominant, more acidic, peptide binding protein of approximately 72 kDa is separated from both TAP subunits (71 and 75 kDa, not separated in the first dimension due to the hydrophobicity of their transmembrane regions). A Western blot similar to that described was probed with specific antibodies to determine the identities of the photoaffinity-labeled 61 and 72 kDa peptide-binding proteins. The 61 kDa protein was confirmed as the previously identified peptide-binding protein PDI, thereby verifying its status as the strongest acceptor of TAP-translocated peptides in the ER (*13*, *14*). The 72 kDa peptide-binding protein was found to exactly comigrate with another member of the thioredoxin superfamily, ERp72 (Figure 3A). Like PDI, this ER-luminal chaperone can influence disulfide-bridge formation (*53*, *54*), but has been shown to associate with misfolded proteins as well (*50*).

Previously, it has been reported that β-estradiol can inhibit the binding of peptides to PDI (*13*, *55*). To test whether peptide binding to ERp72 is equally sensitive to this treatment, as may be suggested by its relation to PDI, β-estradiol was added to T3 microsomes prior to peptide translocation and photoaffinity labeling. Whereas addition of β-estradiol resulted in a clear reduction in the level of photoaffinity labeling of PDI, peptide binding to ERp72 was not influenced by this treatment (Figure 3B), indicating that the substrate-binding sites of PDI and ERp72 have different characteristics.

The Primary Structure but Not the Length of a Peptide Substrate Influences Binding to ER-Resident Peptide Binding Proteins. In addition to the previously identified chaperones PDI, calreticulin, and gp96, we have now identified the chaperones grp170, calnexin, and ERp72 as ER-luminal peptide-binding proteins. These chaperones assist protein folding by temporarily interacting with a (poly)peptide

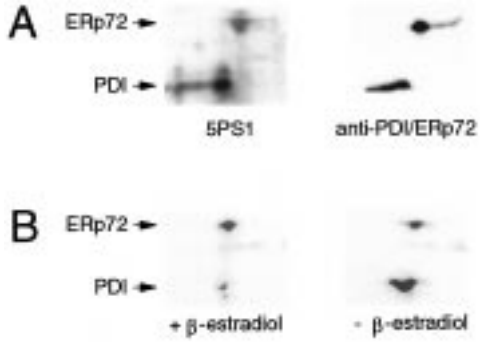

FIGURE 3: ERp72 is an acceptor for TAP-translocated peptides. (A) After TAP translocation of radioiodinated peptides (5PS1 being ERYNKSE-Bpa-L) into T3 microsomes, peptide-bound proteins were photoaffinity labeled by UV exposure. Subsequently, the microsomal proteins were separated by 2D-IEF/SDS−PAGE, followed by a transfer to nitrocellulose. After visualization of the photoaffinity-labeled proteins by phosphoimaging, a part of the filter containing the 61 and 72 kDa peptide-binding proteins was excised (panel 5PS1), and probed with antibodies against candidate proteins. Probing the filter with specific antibodies confirmed the identity of the 61 kDa protein as PDI, and the 72 kDa protein was identified as ERp72 [panel anti-PDI/ERp72 (compilation of the two signals)]. (B) Peptide binding to PDI and ERp72 has different characteristics. The only peptide binding to PDI is affected by β-estradiol. Peptides were translocated into ER microsomes and UV-exposed in the presence or absence of β-estradiol as indicated. The preparations for panel $-\beta$-estradiol included the solvent DMSO. The positions of PDI and ERp72 are denoted.

substrate in the processes of folding. ER-resident chaperones, either soluble (i.e., calreticulin, PDI, gp96, ERp72, and grp170) or membrane-bound (calnexin), are abundantly expressed in the ER lumen (Figure 1B). Since most chaperones interact with unfolded (poly)peptide substrates, certain substrate sequence constraints likely influence their interaction with chaperones and may dictate the differences in chaperone functioning. To investigate substrate selectivities of the identified chaperones, we have used partially degenerated peptides, which vary in length or sequence.

MHC class I molecules preferentially bind peptides of around 9 amino acids. To determine whether peptide binding to ER-resident chaperones is restricted as such, we have determined size selectivities of the photoaffinity-labeled proteins with peptide substrates ranging from 8 to 20 amino acids. To exclude potential effects of sequence selectivities on peptide−chaperone interactions, the peptide substrates that were used were partially degenerated, with a mixture of K, D, F, A, and T (see Table 1). These amino acids represent the different chemical groups of amino acids (basic, acidic, aromatic, hydrophobic, and polar, respectively), with the exception of P. In these peptides, the tyrosine (for iodination) and the photoreactive Bpa group are situated near the opposing N- and C-termini to circumvent visualization of chaperone interactions with peptide degradation intermediates. Although the efficiency of photoaffinity labeling generally decreases with increasing peptide lengths, due to the less efficient peptide translocation of long peptides via TAP, no effect on substrate binding is observed with peptides varying from 8 to 20 amino acids (Figure 4). Longer peptides (30- and 40mer) were very poorly translocated by TAP into the ER, but were found to associate with the same set of chaperones as well (data not shown). The lack of tight restrictions in binding peptides of defined length suggests

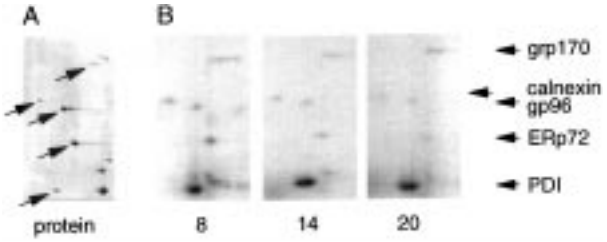

FIGURE 4: Substrate length selectivity of ER-resident chaperones. (A) Separation of T3 microsomal proteins by 2D-IEF/SDS−PAGE, followed by silver staining. The arrows denote the respective photoaffinity-labeled proteins shown in panel B. (B) T3 microsomes were incubated in the presence of ATP with partially degenerated peptides ranging from 8 to 20 amino acids (6PS2A−F) followed by photoaffinity labeling. After separation of the microsomal proteins by 2D-IEF/SDS−PAGE, the peptide-bound proteins were analyzed by phosphoimaging. The peptide-binding chaperones are denoted with arrows on the right. Note the general decrease of the extent of peptide binding with increasing length of the peptide substrates.

that ER chaperones do not bind peptide substrates at a specific peptide-binding site, as found for MHC class I molecules. More likely, peptides bind in general ER chaperones at the same site where nascent polypeptide chains associate, as has recently been shown for PDI (*56*).

Since the length of the peptide substrate does not significantly affect binding to peptide-binding chaperones, we have used photoreactive 9mer peptides to compare influences of amino acid sequence on peptide−chaperone interactions, because they are optimal for peptide translocation via TAP. Experiments similar to those described above were performed with a set of partially degenerated 9mer peptides that have either a K, D, F, L, or T incorporated at positions 2 and 9, as representatives of the different amino acid chemical groups (see Table 1). After photoaffinity labeling and separation by 2D-IEF/SDS−PAGE, the radioactivity associated with the different peptide-binding proteins (corresponding to the amount of peptides bound) was visualized and quantitated by phosphoimaging (Figure 5). As an arbitrary internal reference for peptide binding, the signal of peptide-bound PDI was set at 100%. As stated, PDI is the most dominant peptide-binding protein. All other chaperones are 12-fold (ERp72 for peptides with K at positions 2 and 9) to more than 20-fold less efficient in peptide capture. Notable are the relative differences in the extents of peptide binding of ER-resident chaperones, obtained with peptide substrates that have only limited alterations. grp170 poorly associates with relatively basic peptides, whereas ERp72 does not favor binding of relative acidic and aromatic peptides.

In comparison, silver staining of T3 microsomal proteins suggests that the studied chaperones are all major constituents of the ER lumen (Figures 1B and 4A). Quantification of a similar 2D-IEF/SDS−PAGE gel after Coomassie staining revealed that the expression levels of PDI and calnexin are comparable (as a percentage of the level of PDI expression, calnexin, 109%). grp170 (30%) is expressed at a much lower level in these cells, whereas molar levels of gp96 (153%) and especially ERp72 (385%) are much higher than those of PDI. Correlating peptide binding and the corresponding expression patterns of the different chaperones yields the efficiency of peptide binding at a per molecular basis. Then it appears that ERp72 binds peptides rather poorly, whereas

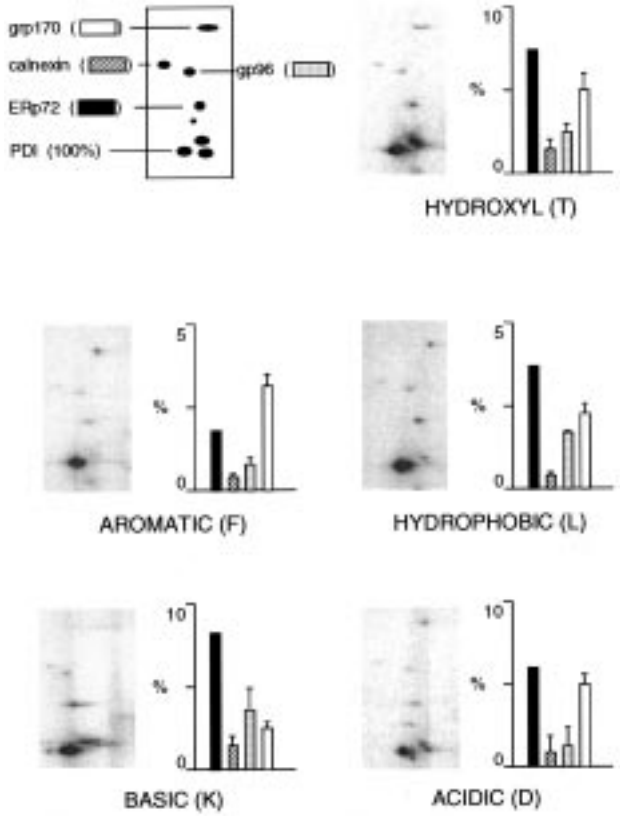

FIGURE 5: Analysis of substrate sequence selectivities of ER-resident peptide-binding chaperones. To analyze the influence of substrate sequence on peptide binding to ER-resident chaperones, T3 microsomes were incubated with different partially degenerated 9mer peptide substrates (6PS3−7), in the presence of ATP, followed by photoaffinity labeling. Microsomal proteins were separated by 2D-IEF/SDS−PAGE and peptide-bound proteins visualized by phosphoimaging. Either a K, D, F, L, or T was systematically introduced at positions 2 and 9 as representatives for the different chemical groups of amino acids. These are denoted under the different panels. The positions of the peptide-binding proteins are depicted in the top left panel. Between brackets are indicated the bar patterns that represent the different peptide-binding chaperones in the graphs. The graphs represent the amount of radioactivity, which correlates with the amount of peptide bound, associated with the different peptide-binding chaperones. The radioactivity of PDI is set at 100%. Error bars represent the variation of two independent experiments.

grp170 binds peptides relatively efficiently. In fact on a molecular basis, grp170 binds peptides approximately 3 (relatively acidic peptides) to 25 times (relatively aromatic peptides) more efficiently than ERp72. Similarly, gp96 binds peptides on average 2 times more efficiently than calnexin, with the exception of relatively hydrophobic peptides (Figure 5). This closely reflects their relative expression patterns in the ER lumen.

ATP Does Not Influence the Chaperone−Peptide Interactions That Were Studied. Several chaperones, including HSP70 and BiP, depend on ATP hydrolysis for their interaction with substrates, whereas others seem to function independent of ATP (*57*). We have determined the role of ATP in the interaction between peptides and the chaperones that were studied. Since our experimental model requires ATP for the introduction of peptides into the ER lumen via TAP, the role of ATP was measured via its capacity to stimulate the off-rate of peptides from the chaperones. After peptide translocation of peptide 5PS2 into T3 microsomes,

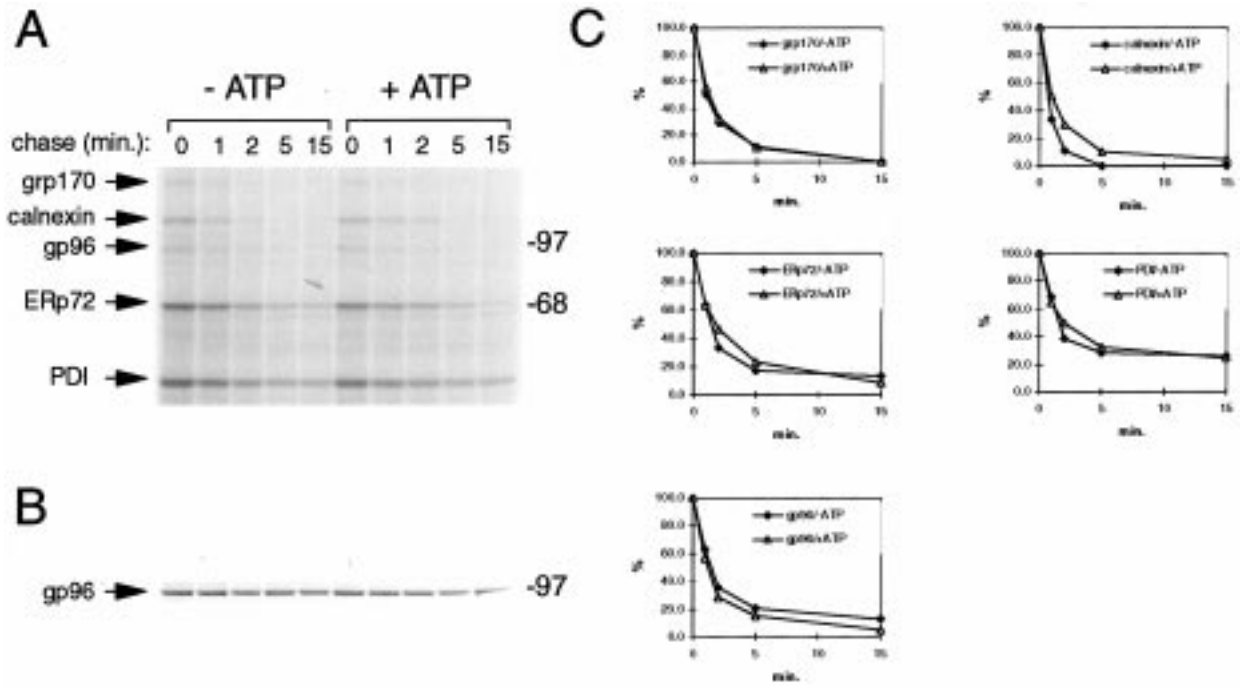

FIGURE 6: Release of peptide substrates in the absence or presence of ATP. (A) T3 microsomes were incubated with peptide 5PS2 in the presence of ATP. After 15 min, the reaction mixture was split and nontranslocated peptides were removed by pelleting the microsomes and subsequent washing. To analyze the influence of ATP on the interaction between peptides and chaperones, the reaction mixtures were chased at 37 °C, either in the absence (−ATP) or in the presence (+ ATP) of 10 mM ATP, for various periods of time as indicated. Subsequently, the released peptides were removed and the peptide-bound proteins photoaffinity-labeled by UV exposure. Microsomal proteins were separated by SDS−PAGE and peptide-bound proteins visualized by autoradiography. (B) Coomassie-stained part of the gel shown in panel A containing gp96. No obvious loss of microsomes is observed during the chase. (C) Quantitative comparison of the effect of ATP on peptide release by the chaperones that were studied. The gel shown in panel A was visualized by phosphoimaging, and the signals of peptide interactions with the various proteins were quantitatively analyzed using TINA 2.09 software. In the graphs, the residual peptides, as a percentage of interaction at time zero, are plotted against the various time points of the chase. The different proteins, and presence or absence of ATP, are denoted in the different graphs. The figure shows one example of two independent experiments with identical results.

and subsequent removal of free peptides and ATP by extensive washing, the reaction mixture was split and chased at 37 °C for up to 15 min either in the absence or in the presence of 10 mM ATP. At the respective time points of the chase, released peptides were removed by washing and microsomal proteins separated by SDS−PAGE after photoaffinity labeling (Figure 6A). Quantitative analyses of the peptide release by the different chaperones do not reveal obvious effects of ATP (Figure 6C). Peptides are rapidly released by most ER chaperones with the exception of PDI, which seems to release its substrates more slowly. The slower off-rate for PDI provides an explanation for why this protein captures peptides so efficiently in the lumen of the ER.

DISCUSSION

The ER lumen is an environment of continuous protein import and export. Nascent proteins enter the ER via the sec61p complex and are stabilized and folded in the ER lumen prior to further transport to the Golgi apparatus (*58*). When proper folding fails, misfolded proteins are targeted for degradation by the proteasome (*59*, *60*). All these processes require the support of molecular chaperones, whose diverse family members are major constituents of the ER lumen (*61*, *62*). Small protein fragments, peptides ranging from 9 to more than 40 amino acids, are translocated into the ER via TAP (*7*−*9*). MHC class I molecules bind a subset of these peptides, which is a requirement for their transport to the cell surface. Subsequently, these peptides are presented to the immune system that thereby encounter a blueprint of the intracellular protein subset. However, in contrast to MHC class I, TAP is not very substrate-selective in its activity (*5*, *37*, *63*, *64*). As a consequence, only a subset of TAP-translocated peptides will be bound by MHC class I molecules. The remainder of these peptides is either trimmed or degraded (*3*, *43*). Since peptidase activity in the ER is very poor (*43*), the majority of the peptides is likely transported back into the cytosol in a TAP-independent manner (*3*, *43*), which may require the involvement of chaperones.

Previously, it was was shown, using photoreactive peptide substrates, that PDI is the most dominant acceptor of peptide substrates in the ER lumen (*13*, *14*). In addition, calreticulin, gp96, and two unidentified ER-luminal proteins, termed gp120 and gp170, were shown to bind peptides as well (*14*). We have now identified gp120 and gp170 as the ER-luminal chaperones calnexin and grp170, respectively. Furthermore, we show that ERp72 efficiently binds peptides in the lumen of the ER. Initially, peptide binding to ERp72 was not observed by SDS−PAGE, since it comigrates with the strongly peptide-binding subunits of TAP. Thus, in analogy with (partially) unfolded nascent polypeptides, TAP-translocated peptides that do not bind MHC class I molecules can associate with a specific subset of ER-resident chaperones that are supposed to play a role in the quality-control apparatus of the ER. The question of whether these ER-resident chaperones indeed are accessory in the removal and/or degradation of peptides in the ER remains to be answered.

Chaperones have to interact physically with their substrates to assist in protein folding. The ER-resident chaperones calnexin, and its soluble homologue calreticulin, have been reported to recognize substrates via monoglucosylated N-linked glycans (*24*, *65*). Previously, we have reported that calreticulin indeed exclusively associates with glycosylated peptide substrates (*14*). In contrast, here we show that calnexin can associate with nonglycosylated peptides as well. This suggests that calnexin, in addition to N-linked glycans, can also recognize (poly)peptide sequences. Other chaperones have been reported to recognize (partially) unfolded proteins as well. BiP, a major hsp70-like chaperone in the ER, has been shown to recognize alternating hydrophobic sequences (*28*). Our peptide substrates lack such sequences. Therefore, BiP is not labeled in our studies, which verifies the specificity of our approach. In contrast, its ER relative grp170 efficiently binds the limited sets of peptides that were used. Although the individual peptide binding characteristics of each of these chaperones awaits more detailed analysis, our data suggest that these two ER-resident hsp70 family members exhibit some nonoverlapping peptide binding characteristics. Striking is the observed peptide binding of grp170 independent of ATP, which is in contrast with ATP-dependent substrate binding of other hsp70 family members.

The chaperones studied may have specific peptide binding sites, like MHC class I molecules. However, the absence of tight restrictions in binding peptides of certain lengths suggests that peptides in general bind chaperones at a site where normally unfolded proteins associate, as has been reported for PDI (*56*). In general, the stability of the observed interactions does not seem to depend on the presence of ATP, since the off-rate of a 9mer model peptide from the chaperones that were studied is not accelerated by addition of exogenous ATP. The peptide off-rate is remarkably lower for PDI which may explain the observed efficiency in the peptide binding of this molecule. Using a relatively small set of partially degenerated 9mer peptides, with selected amino acids at defined positions (position 2 and the C-terminus, corresponding to the most common MHC class I anchor residues) allowed us to visualize differences in the relative substrate binding of ER chaperones. In comparison with the other chaperones that were studied, ERp72 does not prefer peptides when they contain aromatic or acidic amino acids at positions 2 and 9. Similarly, grp170 does not favor relatively basic substrates. Closer examination shows more subtle variations in substrate selectivity; however, more extensive sets of peptides have to be tested to define the exact substrate specificity of the various ER-resident chaperones. The selectivity for gp96 and calnexin differs from that previously published. The exact reasons are not understood, and the source of microsomes used in this study (T3 cells) is the only difference with the previously published experiments (LCL cells). These differences cannot be attributed to the specificity of the TAP transporter in the microsomes. gp96 and calnexin are capable of binding peptides with charged residues at positions 2 and 9. However, in this study, we relate the peptide binding specificity of the different chaperones to the amount of peptides bound by PDI. Since PDI has a preference for relatively hydrophobic peptides (*66*), this relative comparison may underestimate the level of binding of such peptides to the other chaperones identified. Therefore, the experiments presented here only allow conclusions about relative peptide binding within the ER, and not about absolute statements about whether a certain chaperone more efficiently associates with a relatively hydrophobic or charged substrate.

The identification and characterization of novel peptide-binding proteins may have important implications for the development of peptide-vaccination strategies. Previously, it has been shown that tumor-isolated gp96 enables vaccination of mice against a model tumor (*67*, *68*). gp96 is not antigenic and presumably permits vaccination by efficient introduction of associated antigenic peptides into the host MHC class I pathway (*69*). Indeed, immunogenic peptides have been eluted from purified gp96 (*10*), and we and others have recently shown that gp96 is able to directly interact with peptides in the ER (*12*, *14*). These data suggest that gp96 is a potent peptide vehicle for exogenous introduction of antigenic peptides in the host MHC class I pathway, thereby provoking a cytotoxic T-cell response against the antigenic peptide that it has encountered in the ER. The mechanisms by which gp96, but also cytosolic chaperones such as HSP70, are able to introduce antigenic peptides in the MHC class I pathway of monocytic subpopulations are largely unknown (*69*). Chaperones as carriers of antigenic peptides will at least largely improve the pharmacokinetics of peptides in vivo. Peptides associated with chaperones will be protected from degradation in the bloodstream, and will not be removed by glomerular filtration in the kidneys. If this is the main contribution of chaperones such as gp96 in peptide-based vaccinations, it is very likely that other peptide-binding chaperones can be applied for vaccination as well. Especially grp170 and PDI are of great interest since both molecules bind peptides considerably more efficiently than gp96. Whether they can be used for similar purposes is currently under investigation.

ACKNOWLEDGMENT

We thank T. Luts for numerous iodinations and Drs. J. C. Vos, A. Neisig, and A. Benham for helpful suggestions and critical evaluation of the manuscript.

REFERENCES

1. Andrews, D. W., and Johnson, A. E. (1996) *Trends Biochem. Sci. 21*, 365−369.
2. Wilson, I. A. (1996) *Science 272*, 973−974.
3. Schumacher, T. N. M., Kantesaria, D. V., Heemels, M.-T., Ashton-Rickardt, P. G., Shepherd, J. C., Fruh, K., Yang, Y., Peterson, P. A., Tonegawa, S., and Ploegh, H. L. (1994) *J. Exp. Med. 179*, 533−540.
4. Momburg, F., Roelse, J., Hammerling, G. J., and Neefjes, J. J. (1994) *J. Exp. Med. 179*, 1613−1623.
5. Koopmann, J.-O., Post, M., Neefjes, J. J., Hammerling, G. J., and Momburg, F. (1996) *Eur. J. Immunol. 26*, 1720−1728.
6. Rock, K. L., Gramm, C., Rothstein, L., Clark, K., Stein, R., Dick, L., Hwang, D., and Goldberg, A. L. (1994) *Cell 78*, 761−771.
7. Neefjes, J. J., Momburg, F., and Hammerling, G. J. (1993) *Science 261*, 769−771.
8. Shepherd, J. C., Schumacher, T. N. M., Ashton-Rickardt, P. G., Imaeda, S., Ploegh, H. L., Janeway, C. A., Jr., and Tonegawa, S. (1993) *Cell 74*, 577−584.
9. Androlewicz, M. J., Anderson, K. S., and Cresswell, P. (1993) *Proc. Natl. Acad. Sci. U.S.A. 90*, 9130−9134.
10. Nieland, T. J., Tan, M. C., Monne-van Muijen, M., Koning, F., Kruisbeek, A. M., and Van Bleek, G. M. (1996) *Proc. Natl. Acad. Sci. U.S.A. 93*, 6135−6139.

11. Marusina, K., Reid, G., Gabathuler, R., Jefferies, W., and Monaco, J. J. (1997) *Biochemistry 36*, 856−863.
12. Lammert, E., Arnold, D., Nijenhuis, M., Momburg, F., Hammerling, G. J., Brunner, J., Stevanovic, S., Rammensee, H.-G., and Schild, H. (1997) *Eur. J. Immunol. 27*, 923−927.
13. Lammert, E., Stevanovic, S., Brunner, J., Rammensee, H. G., and Schild, H. (1997) *Eur. J. Immunol. 27*, 1685−1690.
14. Spee, P., and Neefjes, J. (1997) *Eur. J. Immunol. 27*, 2441−2449.
15. Koopmann, J. O., Hammerling, G. J., and Momburg, F. (1997) *Curr. Opin. Immunol. 9*, 80−88.
16. Solheim, J. C., Carreno, B. M., and Hansen, T. H. (1997) *J. Immunol. 158*, 541−543.
17. Ortmann, B., Androlewicz, M. J., and Cresswell, P. (1994) *Nature 368*, 864−867.
18. Lindquist, J. A., Jensen, O. N., Mann, M., and Hammerling, G. J. (1998) *EMBO J. 17*, 2186−2195.
19. Morrice, N. A., and Powis, S. J. (1998) *Curr. Biol. 8*, 713−716.
20. Hughes, E. A., and Cresswell, P. (1998) *Curr. Biol. 8*, 709−712.
21. Sadasivan, B., Lehner, P. J., Ortmann, B., Spies, T., and Cresswell, P. (1996) *Immunity 5*, 103 (abstract).
22. Solheim, J. C., Harris, M. R., Kindle, C. S., and Hansen, T. H. (1997) *J. Immunol. 158*, 2236−2241.
23. van Leeuwen, J. E., and Kearse, K. P. (1996) *Proc. Natl. Acad. Sci. U.S.A. 93*, 13997−14001.
24. Rodan, A. R., Simons, J. F., Trombetta, E. S., and Helenius, A. (1996) *EMBO J. 15*, 6921−6930.
25. Zapun, A., Petrescu, S. M., Rudd, P. M., Dwek, R. A., Thomas, D. Y., and Bergeron, J. J. (1997) *Cell 88*, 29−38.
26. Krause, K.-H., and Michalak, M. (1997) *Cell 88*, 439−443.
27. Trombetta, E. S., and Helenius, A. (1998) *Curr. Opin. Struct. Biol. 8*, 587−592.
28. Blond-Elguindi, S., Cwirla, S. E., Dower, W. J., Lipshutz, R. J., Sprang, S. R., Sambrook, J. F., and Gething, M.-J. H. (1993) *Cell 75*, 717−728.
29. Flynn, G. C., Pohl, J., Flocco, M. T., and Rothman, J. E. (1991) *Nature 353*, 726−730.
30. Noiva, R., Freedman, R. B., and Lennarz, W. J. (1993) *J. Biol. Chem. 268*, 19210−19217.
31. Luz, J. M., and Lennarz, W. J. (1996) *EXS 77*, 97−117.
32. Srivastava, P. K., De Leo, A. B., and Old, L. J. (1986) *Proc. Natl. Acad. Sci. U.S.A. 83*, 3407−3411.
33. Palladino, M. A., Jr., Srivastava, P. K., Oettgen, H. F., and DeLeo, A. B. (1987) *Cancer Res. 47*, 5074−5079.
34. Suto, R., and Srivastava, P. K. (1995) *Science 269*, 1585−1588.
35. Srivastava, P. K., Menoret, A., Basu, S., Binder, R. J., and McQuade, K. L. (1998) *Immunity 8*, 657−665.
36. Momburg, F., Roelse, J., Howard, J. C., Butcher, G. W., Hammerling, G. J., and Neefjes, J. J. (1994) *Nature 367*, 648−651.
37. Neefjes, J., Gottfried, E., Roelse, J., Gromme, M., Obst, R., Hammerling, G. J., and Momburg, F. (1995) *Eur. J. Immunol. 25*, 1133−1136.
38. Kauer, J. C., Erickson-Viitanen, S., Wolfe, H. R., Jr., and DeGrado, W. F. (1986) *J. Biol. Chem. 261*, 10695−10700.
39. Lin, H. Y., Masso-Welch, P., Di, Y. P., Cai, J. W., Shen, J. W., and Subjeck, J. R. (1993) *Mol. Biol. Cell 4*, 1109−1119.
40. Hochstenbach, F., David, V., Watkins, S., and Brenner, M. B. (1992) *Proc. Natl. Acad. Sci. U.S.A. 89*, 4734−4738.
41. Salter, R. D., Howell, D. N., and Cresswell, P. (1985) *Immunogenetics 21*, 235−246.
42. Momburg, F., Ortiz-Navarrete, V., Neefjes, J. J., Goulmy, E., Van De Wal, Y., Spits, H., Powis, S. J., Butcher, G. W., Howard, J. C., Walden, P., and Hammerling, G. J. (1992) *Nature 360*, 174−177.
43. Roelse, J., Gromme, M., Momburg, F., Hammerling, G., and Neefjes, J. (1994) *J. Exp. Med. 180*, 1591−1597.
44. Androlewicz, M. J., Ortmann, B., van Endert, P. M., Spies, T., and Cresswell, P. (1994) *Proc. Natl. Acad. Sci. U.S.A. 91*, 12716−12720.
45. Marusina, K., and Monaco, J. J. (1996) *Curr. Opin. Hematol. 3*, 19−26.
46. Chen, X., Easton, D., Oh, H. J., Lee-Yoon, D. S., Liu, X., and Subjeck, J. (1996) *FEBS Lett. 380*, 68−72.
47. Craven, R. A., Tyson, J. R., and Stirling, C. J. (1997) *Trends Cell Biol. 7*, 277−282.
48. Dierks, T., Volkmer, J., Schlenstedt, G., Jung, C., Sandholzer, U., Zachmann, K., Schlotterhose, P., Neifer, K., Schmidt, B., and Zimmermann, R. (1996) *EMBO J. 15*, 6931−6942.
49. Ou, W.-J., Cameron, P. H., Thomas, D. Y., and Bergeron, J. J. M. (1993) *Nature 364*, 771−776.
50. Kuznetsov, G., Chen, L. B., and Nigam, S. K. (1997) *J. Biol. Chem. 272*, 3057−3063.
51. David, V., Hochstenbach, F., Rajagopalan, S., and Brenner, M. B. (1993) *J. Biol. Chem. 268*, 9585−9592.
52. Zhang, J. X., Braakman, I., Matlack, K. E., and Helenius, A. (1997) *Mol. Biol. Cell 8*, 1943−1954.
53. Rupp, K., Birnbach, U., Lundstrom, J., Van, P. N., and Soling, H. D. (1994) *J. Biol. Chem. 269*, 2501−2507.
54. Lundstrom-Ljung, J., Birnbach, U., Rupp, K., Soling, H. D., and Holmgren, A. (1995) *FEBS Lett. 357*, 305−308.
55. Tsibris, J. C. M., Hunt, L. T., Ballejo, G., Barker, W. C., Toney, L. T., and Spellacy, W. N. (1989) *J. Biol. Chem. 264*, 13967−13970.
56. Klappa, P., Ruddock, L. W., Darby, N. J., and Freedman, R. B. (1998) *EMBO J. 17*, 927−935.
57. Hartl, F. U. (1996) *Nature 381*, 571−579.
58. Sakaguchi, M. (1997) *Curr. Opin. Biotechnol. 8*, 595−601.
59. Sommer, T., and Wolf, D. H. (1997) *FASEB J. 11*, 1227−1233.
60. Kopito, R. R. (1997) *Cell 88*, 427−430.
61. Hayes, S. A., and Dice, J. F. (1996) *J. Cell Biol. 132*, 255−258.
62. Plemper, R. K., Bohmler, S., Bordallo, J., Sommer, T., and Wolf, D. H. (1997) *Nature 388*, 891−895.
63. Neisig, A., Roelse, J., Sijts, A. J. A. M., Ossendorp, F., Feltkamp, M. C. W., Kast, W. M., Melief, C. J. M., and Neefjes, J. J. (1995) *J. Immunol. 154*, 1273−1279.
64. Androlewicz, M. J., and Cresswell, P. (1996) *Immunity 5*, 1−5.
65. Hebert, D. N., Foellmer, B., and Helenius, A. (1995) *Cell 81*, 425−433.
66. Klappa, P., Hawkins, H. C., and Freedman, R. B. (1997) *Eur. J. Biochem. 248*, 37−42.
67. Srivastava, P. K., Udono, H., Blachere, N. E., and Li, Z. (1994) *Immunogenetics 39*, 93−98.
68. Tamura, Y., Peng, P., Lui, K., Daou, M., and Srivastava, P. K. (1997) *Science 278*, 117−120.
69. Nicchitta, C. V. (1998) *Curr. Opin. Immunol. 10*, 103−109.

BI990321R